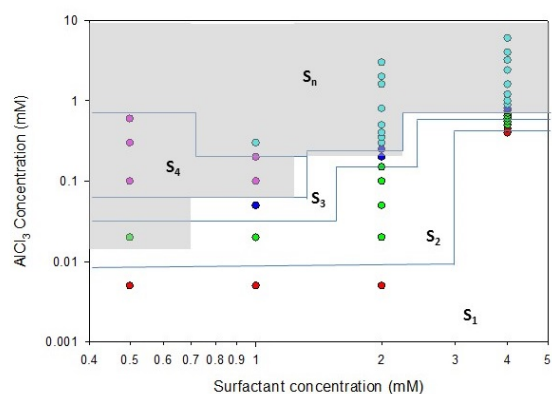
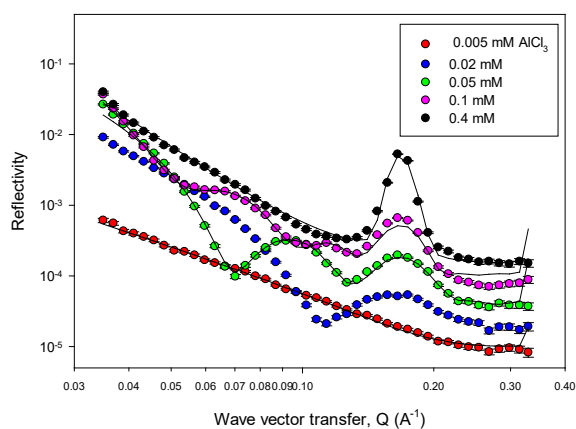


TOC GRAPHIC

The impact of electrolyte on the adsorption of the anionic surfactant methyl ester sulfonate at the air-solution interface: surface multilayer formation.

H Xu, R K Thomas, J Penfold, P X Li, K Ma, R J L Welbourne, D W Roberts, J T Petkov



The impact of electrolyte on the adsorption of the anionic surfactant methyl ester sulfonate at the air-solution interface: surface multilayer formation

H Xu¹, R K Thomas², J Penfold^{2,3}, P X Li³, K Ma³, R J L Welbourne³, D W Roberts⁴, J T Petkov^{1#}

1. KLK Oleo, SDN BHD, Menara KLK, Muliara Damansara, 47810, Petaling, Jaya Selanger, Malaysia
2. Physical and Theoretical Chemistry Laboratory, Oxford University, South Parks Road, Oxford, UK
3. ISIS Facility, STFC, Rutherford Appleton Laboratory, Chilton, Didcot, OXON, UK
4. D W Roberts, School of Pharmacy and Biomolecular Sciences, Liverpool John Moores University, Byrom Street, Liverpool, L3 3AF, UK

Current Address: Lonza UK, GB-Blackley, Manchester, M9 8ES, UK

Corresponding Author: Professor Jeff Penfold, phone: +44 1235 445681, email: jeff.penfold@stfc.ac.uk

Keywords: Methyl ester sulfonate adsorption, surface tension, neutron reflectivity, air-water interface, surface multilayers.

ABSTRACT

The methyl ester sulfonates represent a promising group of anionic surfactants which have the potential for improved performance and biocompatibility in a range of applications. Their solution properties, in particular their tolerance to hard water, suggests that surface ordering may occur in the presence of multi-valent counterion. Understanding their adsorption properties in a range of different circumstances is key to the exploitation of their potential.

Neutron reflectivity and surface tension have been used to characterise the adsorption at the air-aqueous solution interface of the anionic surfactant sodium tetradecanoic 2-sulfo 1-methyl ester, C₁₄MES, in the absence of electrolyte and in the presence of mono, di, and tri-valent counterions, Na⁺, Ca²⁺, and Al³⁺. In particular the emphasis has been on exploring the tendency to form layered structures at the interface.

In the absence of electrolyte and in the presence of NaCl and CaCl₂ and AlCl₃ at low concentrations monolayer adsorption is observed, and the addition of electrolyte results in enhanced adsorption. In the presence of NaCl and CaCl₂ only monolayer adsorption is observed. However at higher AlCl₃ concentrations surface multilayer formation is observed, in which the number of bilayers at the surface depends upon the surfactant and AlCl₃ concentrations.

INTRODUCTION

Anionic surfactants are the major surface active ingredient in a wide range of home and personal care products (1, 2). Improved performance has invariably involved formulations using multicomponent mixtures, and notably anionic / nonionic surfactant mixtures (3, 4). However, over a long period the structure of the anionic surfactants has also evolved to provide improved hard water characteristics, improved detergency, enhanced performance at lower temperatures and improved biocompatibility and biodegradability (1, 2). This has led to the development of the alkyl benzene sulfonates, LAS, (5), and the alkyl ethoxy ether sulfates, SLES, (6) from the simpler alkyl sulfates (7). The alkyl sulfates, especially as the alkyl chain length increases, rapidly precipitate due to the strong binding and complexation with the multivalent ions in hard water (8-12). Coadsorption and self-assembly with a nonionic cosurfactant can partially mitigate such effects (8). However the alkyl benzene sulfonates (2) and alkyl ethoxy ether sulfates (5, 13-15) have a much greater tolerance to precipitation in the presence of multivalent ions, and LAS also demonstrates improved detergency properties and biodegradability (1, 2).

More recently it has been demonstrated that the methyl ester sulfonates, MES surfactants have potential as replacements for the anionic surfactants such as LAS (16, 17). Recent studies have shown that MES has better cold water detergency, better hard water tolerance and is more biodegradable than LAS (18-22). Synthesised from sources such as sustainable palm oil and the increased availability of other MES feedstocks such as the bi-products from bio-diesel production (23), and potential low production costs, make it an increasingly environmentally attractive option. Hence the synthesis and purification of MES has been extensively studied and reported (24-26). However, in contrast, the basic physicochemical properties of MES, notably its adsorption and self-assembly, have been less extensively studied (27, 28).

To address this paucity of data we have recently studied the adsorption characteristics of C₁₄MES (29), from the evaluation of surface tension, ST, and neutron reflectivity, NR, data. The main focus of this paper is on the impact of multivalent ions on the surface adsorption and on the structure of the adsorbed layer of MES. Recently it has been extensively demonstrated with LAS and SLES that the addition of multivalent counterions results in the formation of surface multilayer structures at low surfactant concentrations and outside the regime of precipitation (30-36). An important characteristic feature of such surface multilayer formation

is the onset of extreme and persistent wetting of hydrophobic surfaces (37). In particular surface multilayer formation has been demonstrated with different LAS isomers and LAS / nonionic surfactant mixtures with the addition of Ca^{2+} , and for SLES with the addition of Al^{3+} ions. Such surface structures also offer great potential for improved detergency and enhanced delivery / retention at surfaces of a range of co-active ingredients (38). The strong counterion binding promotes the adsorption of a concentrated lamellar phase from a dilute solution, and can be considered as a surface induced phase or likened to a wetting or pre-wetting transition (39). The improved solubility of this type of anionic surfactant in the presence of multivalent ions and their tolerance to precipitation are features associated with their tendency to the formation of surface multilayer structures. It is evident that the MES surfactant possesses many of those characteristics and we report here the formation of surface multilayer structures for MES in the presence of Al^{3+} counterions.

EXPERIMENTAL DETAILS

(i) Surface Tension

The surface tension, ST, measurements were made using a Kruss K100 maximum pull tensiometer, using a platinum plate. The plate was rinsed in high purity water and dried in a Bunsen flame before each measurement. The temperature was controlled at $25 \pm 0.5^\circ\text{C}$ and the solutions partially covered to minimise evaporation. At each concentration repeated measurements were made, ~ 5 to 10 repeats, and the variation in ST was ≤ 0.2 mN/m. The values plotted are the average of the repeated measurements, and the associated error is ≤ 0.1 mN/m. The ST measurements were made on the hydrogeneous surfactant in H_2O .

(ii) Neutron Reflectivity

The neutron reflectivity, NR, measurements were made on the INTER reflectometer (40) at the ISIS pulsed neutron source. The reflectivity, $R(Q)$, is measured as a function of the wave vector transfer, Q , perpendicular to the surface; where Q is defined as $Q=4\pi\sin\theta/\lambda$, θ is the grazing angle of incidence and λ the neutron wavelength. The measurements were made at a fixed θ of 2.3° and a λ range of 1 to 15 Å, to cover a Q range ~ 0.03 to 0.3 Å^{-1} .

The reflectivity was normalised to an absolute scale by reference to the direct beam intensity and the reflectivity from a D_2O surface. The measurements were all made in null reflecting water, nrw, (8 mole % D_2O / 92 mole % H_2O , with a scattering length density, ρ , of 0.0 and so index matched to air) using deuterium labelled surfactants. The measurements were made in

sealed Teflon troughs, with sample volumes ~ 25 mL, and at a temperature of $25 \pm 0.5^\circ\text{C}$. Each measurement took ~ 20 to 30 mins and the measurements were made sequentially on a 7 position sample changer. Each measurement was repeated ~ 2 to 3 times until the reflectivity profile had reached a steady state, over a total lapse time ~ 3 to 6 hours.

Through the kinematic approximation (41) the reflectivity is related to the square of the Fourier transform of the scattering length density distribution, $\rho(z)$, normal to the surface, in the z direction; and where $\rho(z)$ is defined as $\rho(z) = \sum_i b_i n_i(z)$, $n_i(z)$ is the number density of species i and b_i its neutron scattering length, such that,

$$R(Q) = \frac{16\pi^2}{Q^2} \left| \int \rho(z) e^{-iQz} dz \right|^2 \quad (1)$$

$\rho(z)$ can be manipulated using D/H isotopic substitution, as the neutron scattering lengths of H and D are quite different, -3.75×10^{-6} and 6.67×10^{-5} Å respectively. For the measurement of a deuterium labelled surfactant adsorbed at the air-water interface this provides a direct evaluation of the adsorbed amount and the structure of the adsorbed layer, as demonstrated in a wide range of surfactant (41) and polymer / surfactant mixtures (42).

(iii) Materials.

The sodium tetradecanoic 2-sulfo 1-methyl ester, C_{14}MES , with a chemical formula $\text{CH}_3(\text{CH}_2)_{11}\text{CH}(\text{SO}_3\text{Na})\text{COOCH}_3$ (see figure 1) was synthesised and purified in two forms, with and without the alkyl chain deuterium labelled. The synthesis and purification of the C_{14}MES is described in detail elsewhere in a precursor paper to this paper (29).

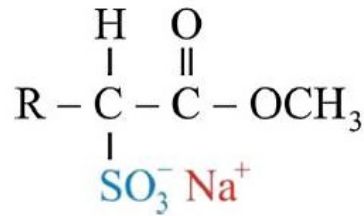


Figure 1. Generic structure of MES surfactant, the group labelled R is $\text{CH}_3(\text{CH}_2)_{11}$ for C_{14}MES .

The hydrogenous and deuterium labelled C_{14}MES are referred to as h- C_{14}MES and d- C_{14}MES respectively.

Deuterium oxide, D₂O, was obtained from Sigma-Aldrich, and high purity water (Elga Ultrapure with a resistivity of 18.2 MCcm) was used throughout. Analytical grade (>99.9% purity) AlCl₃, NaCl and CaCl₂ were obtained from Sigma-Aldrich and used as supplied. All glassware, Teflon troughs and other containers used for the NR and ST measurements and sample preparation were cleaned in alkali detergent (Decon 90) and extensively rinsed in Ultrapure water.

(iv) Measurements made

ST measurements were made for h-C₁₄MES in H₂O, in 0.1 M NaCl and in AlCl₃ solutions at concentrations of 0.1 to 0.3 mM.

NR measurements were made for d-C₁₄MES in nrw over a concentration range of 0.05 to 15 mM, in order to establish the nature of the adsorption isotherm and are discussed in detail elsewhere (29). At a surfactant concentration of 2 mM, for d-C₁₄MES, measurements were made in CaCl₂, in the CaCl₂ concentration range from 0.5 to 6 mM. Measurements were made for 5 mM d-C₁₄MES in 0.1 M NaCl and also at 5mM surfactant concentration for a 50/50 mole ratio mixture of d-C₁₄MES / h-C₁₄MES. In the presence of AlCl₃ measurements were made for d-C₁₄MES at 4mM and AlCl₃ concentrations from 0.4 to 6 mM, at 2mM and AlCl₃ concentrations from 0.005 to 3 mM, at 1 mM and AlCl₃ concentrations from 0.005 to 0.6 mM, and at 0.5 mM and AlCl₃ concentrations from 0.005 to 0.6 mM.

RESULTS and DISCUSSION

(i) Surface Tension data

Figure 2 shows the surface tension data for h-C₁₄MES in H₂O, in 0.1M NaCl and in 0.3 mM AlCl₃. From figure 2 the cmc's in the absence of electrolyte, in 0.1M NaCl, and in 0.3 mM AlCl₃ are 2.4 mM, 0.34 mM, and 0.23 ±0.03 mM respectively. In H₂O the surface tension at the cmc is ~ 40.0 mN/m. The addition of electrolyte reduces the values of the cmc and the ST at the cmc, and the trivalent Al³⁺ is much more effective in that reduction.

There is some variability in the reported values of the critical micelle concentration, cmc, for the MES surfactants, and this in part reflects the presence of impurities and variations in the surfactant structure, alkyl chain length and degree of esterification. Ohbu et al (27) report a cmc for C₁₄MES of 2.8 mM at 13°C, and demonstrate the decrease in the cmc with the size of the ester group and the alkyl chain length; although the method of determination is not stated

it is assumed to be from ST data. Jin et al (43) report variations in the ST and cmc, the cmc varying from 5.0 to 5.5 mM and ST values at the cmc in range 31.5 to 32.5 mN/m, depending upon the source of the waste cooking oils used in the synthesis. Wong et al (28), in their study of the binary mixtures of MES and the cationic alkyl trimethylammonium bromides, report a cmc value for C₁₄MES of 2.71 mM. Danov et al (16) remarked on the large variation in the reported cmc values for the MES surfactants in the literature, which they ascribe to impurities. They measured the cmc for C₁₄ to C₁₈MES by ST and conductivity. From ST the cmc for C₁₄MES in 10 mM NaOH was \sim 1mM, whereas from conductivity it was \sim 3.68 mM. Both values are at variance with the data presented here and the implications have been discussed in more detail elsewhere (29). However, the ST results presented here are in broad agreement with results of Ohbu et al (27) and Wong et al (28).

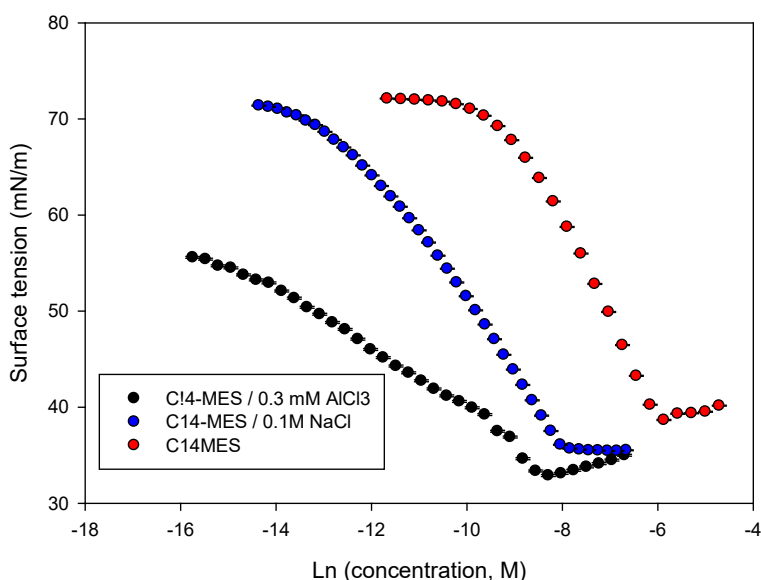


Figure 2. Surface tension data for *h*-C₁₄MES in H₂O (●), 0.1M NaCl (●), and 0.3 mM AlCl₃ (●).

The addition of electrolyte, as expected, results in a shift in the cmc to lower surfactant concentrations, and a slight reduction in the ST at the cmc. The effects are much more pronounced for the addition of 0.3 mM AlCl₃ than for the addition of 100 mM NaCl; as expected from previous studies on the impact of Al³⁺ on the anionic surfactant SLES (34, 35). With the addition of Al³⁺ the variation in ST with surfactant concentration at low surfactant concentrations is more gradual, and the absolute values are much lower. At the cmc there is a minimum at a ST value \sim 30 mN/m. The ST then increases towards the value measured at

higher surfactant concentrations in the absence of electrolyte. The variation, as previously discussed for SLES (34, 35), arises due to the measurements being made at a fixed small AlCl_3 concentration, which is initially comparable to the surfactant concentration, but rapidly becomes \ll surfactant concentration at concentrations \geq cmc.

(ii) Monolayer adsorption

For a more accurate and unambiguous determination of the adsorption properties in the absence of electrolyte NR measurements have been made for d- C_{14}MES in nrw, and are reported and discussed in detail in a related paper (29).

In the absence of electrolyte monolayer adsorption is observed; and the mean thickness, d , of the adsorbed layer, measured in the concentration range 0.05 to 15 mM, is $\sim 20 \pm 2$ Å. The reflectivity data is analysed as a single layer of uniform composition. The product of the thickness and scattering length density from the analysis, $d\rho$, is directly related to the adsorbed amount of surfactant at the interface (41); such that the area/molecule at the interface, A , is given by,

$$A = \sum b / d\rho \quad (2)$$

and the adsorbed amount, Γ , is $\Gamma = 1/AN_a$, and N_a is Avogadro's number. The $\sum b$ values for d- C_{14}MES and h- C_{14}MES are 2.87×10^{-3} and 2.68×10^{-4} Å respectively. The C_{14}MES adsorption isotherm, determined in this way, is reproduced from reference 29 in figure S1 in the Supporting Information. From 4 to 15 mM C_{14}MES concentration the mean area/molecule is $\sim 49 \pm 1$ Å² and the mean adsorbed amount is $\sim 3.4 \pm 0.10 \times 10^{-10}$ mol cm⁻². For the evaluation of the surfactant adsorption from NR measurements a stringent test of the relative purity and consistency between the d- and h- labelled surfactants is to compare the adsorption determined from the d-surfactant with that obtained from an equimolar mixture of the d- and h-surfactants. This was done here for the 50/50 mixture of d- C_{14}MES and h- C_{14}MES at a surfactant concentration of 5 mM; and within error the adsorbed amount, $\sim 3.4 \times 10^{-10}$ mol cm⁻², is the same as measured for d- C_{14}MES at 4 and 6 mM.

Although a mean value for the adsorption in the concentration range 4 to 15 mM is quoted, as illustrated in figure S1 the adsorbed amount does increase systematically over that range, at the limit of the error in the measurement. This should be expected for anionic surfactants as the degree of dissociation decreases and the surfactant activity increases as the surfactant

concentration increases above the cmc (44). This variation is broadly consistent with that expected for an ionic surfactant. It is indicative of a more weakly anionic surfactant compared to SDS, and comparable to that observed for SLES (44). The variation of the ST in the absence of electrolyte above the cmc (see figure 2), which does not show a systematic decrease, is also consistent with that observation. In contrast for SDS a greater variation in the ST above the cmc is observed (44).

Monolayer adsorption in the presence of NaCl, CaCl₂ and AlCl₃ at low concentrations was measured at some fixed surfactant and electrolyte concentrations. The data for 5 mM C₁₄MES in 100 mM NaCl gives an adsorbed amount $\sim 3.56 \times 10^{-10}$ mol cm⁻², for 2 mM C₁₄MES in 2 mM CaCl₂ $\sim 3.68 \times 10^{-10}$ mol cm⁻², and for 4 mM C₁₄MES in 0.4 mM AlCl₃ $\sim 3.67 \times 10^{-10}$ mol cm⁻². This represents an electrolyte induced increase $\sim 5\%$. In contrast the increase in the adsorbed amount for SDS at the cmc with the addition of 100 mM NaCl is $\sim 23\%$ (44); and for SLES $\sim 16\%$ (44). For SDS this is comparable to the increase observed in the absence of electrolyte as the SDS concentration increases from the cmc to ten times the cmc. NR measurements were also made for 2 mM d-C₁₄MES in CaCl₂, in the concentration range 0.5 to 6.0 mM CaCl₂. Over that CaCl₂ concentration range monolayer adsorption is only observed and the solutions, as observed for all the data where monolayer adsorption occurs, were optically clear. Over the CaCl₂ concentration range explored the adsorbed amount varied from 3.65 to 3.77×10^{-10} mol cm⁻², compared to a value in the absence of electrolyte at 2 mM $\sim 3.2 \times 10^{-10}$ mol cm⁻², with an error $\pm 0.10 \times 10^{-10}$ mol cm⁻².

(iii) Multilayer adsorption

The addition of AlCl₃ to C₁₄MES initially results in monolayer adsorption at extremely low concentrations of AlCl₃, as discussed in the previous section. However, with increasing AlCl₃ concentration the reflectivity changes dramatically and there is a correspondingly rich evolution in the surface structure from monolayer to multilayer structures. The nature of the surface structure and its evolution with AlCl₃ concentration depends upon the surfactant concentration and the relative AlCl₃ concentration. NR measurements were made for a range of AlCl₃ concentrations, from 0.005 to 6 mM AlCl₃ concentration depending upon the C₁₄MES concentration, and at C₁₄MES concentrations of 0.5, 1.0, 2.0 and 4.0 mM.

When monolayer adsorption occurs the adsorption, within the timescale of the sequential measurements, does not vary with time. When multilayer adsorption occurs the reflectivity varies with time, to reach an equilibrium or steady state structure over the timescale associated

with 3 repeated measurements, ~ 180 to 360 minutes. This time variation is shown in figure 3 for 4 mM $C_{14}MES$ / 6 mM $AlCl_3$, and is representative of the variations that occur.

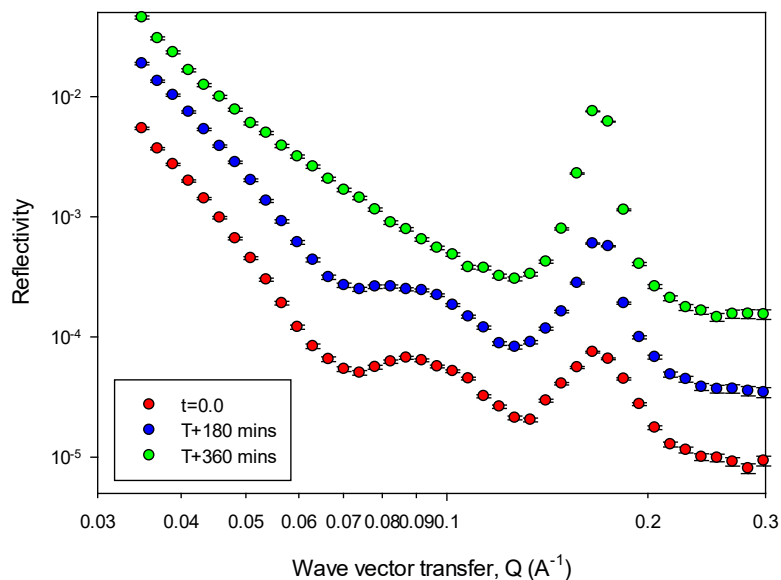


Figure 3. Neutron reflectivity for 4mM $C_{14}MES$ / 6 mM $AlCl_3$, (red) at $t=0$, (blue) + 180 mins, and (green) +360 mins. The data for $t=180$, and 360 mins are shifted vertically by $\times 4$ and $\times 16$ respectively for clarity.

By analogy with the detailed discussion and analysis of the data in figure 4 the surface structure in figure 3 undergoes a transition with time from a multilayer with a finite small number of bilayers, ~ 2 -3, to a multilayer characterised by a single Bragg peak in which the number of bilayers at the interface is large, ≥ 30 . The subsequent data and analysis in figure 4, and the approximate surface phase diagram in figure 5 are based on equilibrium structures.

The NR data at 1 mM $C_{14}MES$ shown in figure 4 encapsulates the equilibrium, or steady state, changes in reflectivity and surface structure that are encountered as the $AlCl_3$ concentration is increased at a fixed $C_{14}MES$ concentration. The NR data are analysed using the optical matrix method adapted for NR (41, 45). The simplest model, that is, the least number of discrete layers required to represent the data, is used. At the lowest $AlCl_3$ concentration, 0.005 mM, the reflectivity is a featureless curve consistent with a single monolayer of surfactant adsorbed at the interface; with an adsorbed layer thickness ~ 20 Å and a scattering length density $\sim 3.2 \times 10^{-6}$ Å⁻². This gives an adsorbed amount $\sim 3.7 \times 10^{-10}$ mol cm⁻², consistent with the previously

measured adsorption data in the absence and presence of electrolyte (44), see previously reported data in figure S1 in the Supporting Information. At an AlCl_3 concentration of 0.02 mM the reflectivity changes form and is dominated by a single broad interference fringe between Q values ~ 0.1 to 0.3 \AA^{-1} . This is best described by three layers, which correspond to the initial monolayer at the interface with a single bilayer beneath the monolayer, as encapsulated by the model parameters in table 1.

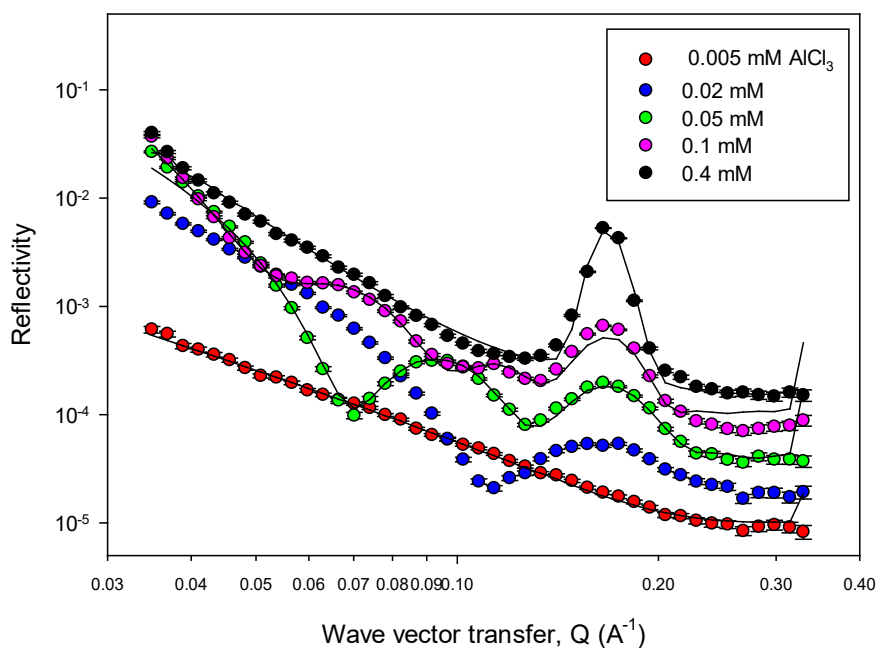


Figure 4. NR data for 1 mM $C_{14}\text{MES}$, for 0.005 mM AlCl_3 (red), 0.05 mM AlCl_3 (green), 0.1 mM AlCl_3 (pink) and 0.4 mM AlCl_3 (black). Each curve is shifted vertically by $\times 2$ for clarity. The solid lines are model calculations as described in the text and for the key model parameters summarised in table 1.

At an AlCl_3 concentration of 0.05 mM the single interference fringe has evolved into a double interference fringe pattern. This is best described by five layers, corresponding to an initial monolayer and two discrete bilayers beneath that monolayer. At the higher AlCl_3 concentrations (0.4 mM) the reflectivity is now dominated by a pronounced Bragg peak at a Q value $\sim 0.16 \text{ \AA}^{-1}$, consistent with a multilayer structure with a bilayer thickness $\sim 38 \text{ \AA}$. In this case the reflectivity is dominated by the multilayer structure, and the contribution from the initial monolayer is less important. For the appearance of a single Bragg peak and no visible interference fringes arising from the total film thickness at the interface, the modelling of the reflectivity is most sensitive to d_t , $\Delta\rho$, and n ; where d_t is the bilayer thickness, $\Delta\rho$ the difference

in the scattering length density of the two regions of the bilayer structure, and n is the number of bilayers. The visibility of the Bragg peak, that is its relative reflectivity, is related to a combination of n and $\Delta\rho$. The lack of interference fringes from the total thickness implies that n is relatively large. The width of the Bragg peak is inversely related to n , but has to be convolved with the instrument resolution, ΔQ . The value of ΔQ in this Q range from purely instrumental factors is ~ 0.05 , but from the detailed analysis of the data (see table 1) ΔQ is generally larger, ~ 0.1 . This is because the surface coverage of multilayer structures is in a form analogous to lamellar crystallites at the surface, and so ΔQ is broadened by the mosaic spread of the surface lamellar patches. In detail, the surface multilayer structure where n is large is more conveniently analysed using a surface multilayer model based on the kinematic approximation (46, 47) and which has been extensively applied to such systems. In this case the key model parameters are the bilayer thickness, d_t , where $d_t = d_1 + d_2$ and d_1 and d_2 are the hydrophobic alkyl chain and hydrated hydrophilic regions of the bilayer, ρ_1 and ρ_2 are their respective scattering length densities, $\Delta\rho$ is $(\rho_1 - \rho_2)$, n is the number of bilayers and ΔQ the resolution terms. The bilayer thickness obtained is $\sim 38 \text{ \AA}$, n is ~ 30 , ΔQ is ~ 0.12 and $\Delta\rho$ is $\sim 1.4 \times 10^{-6} \text{ \AA}^{-2}$ (see table 1 for full details).

Table 1. Key model parameters from analysis of NR data for 1 mM $C_{14}MES$ at $AlCl_3$ concentration of 0.005, 0.02, 0.05, 0.1 and 0.4 mM.

$AlCl_3$ concentr ation (mM)	d_1 (± 1 \AA)	ρ_1 ($\pm 0.$ 05 x 10^{-6} \AA^{-2})	d_2 (± 1 \AA)	ρ_2 ($\pm 0.$ 05 x 10^{-6} \AA^{-2})	d_3 (± 1 \AA)	ρ_3 ($\pm 0.$ 05 x 10^{-6} \AA^{-2})	d_4 (± 1 \AA)	ρ_4 ($\pm 0.$ 05 x 10^{-6} \AA^{-2})	d_5 (± 1 \AA)	ρ_5 ($\pm 0.$ 05 x 10^{-6} \AA^{-2})	d_6 (± 1 \AA)	ρ_6 ($\pm 0.$ 05 x 10^{-6} \AA^{-2})	d_7 (± 1 \AA)	ρ_7 ($\pm 0.$ 05 x 10^{-6} \AA^{-2})
0.005	21	3.24	-	-	-	-	-	-	-	-	-	-	-	-
0.02	26	4.44	5	0.45	20	3.94	-	-	-	-	-	-	-	-
0.05	19	3.22	8	0.72	24. 6	4.1	8.0	0.76	26. 5	4.46	-	-	-	-
0.1	14	3.2	13	0.9	26. 5	2.47	10	0.72	25. 6	5.2	7.5	1.0	26	3.3
	d_1 (± 1 \AA)	ρ_1 ($\pm 0.$ 05 x 10^{-6} \AA^{-2})	d_2 (± 1 \AA)	ρ_2 ($\pm 0.$ 05 x 10^{-6} \AA^{-2})	n	ΔQ								

0.4	21	3.67	16. 5	2.15	30	0.12								
-----	----	------	----------	------	----	------	--	--	--	--	--	--	--	--

The reflectivity at the AlCl_3 concentration of 0.1 mM is intermediate in form between that observed at 0.05 and 0.4 mM. That is, there is a broad Bragg peak at a $Q \sim 0.16 \text{ \AA}^{-1}$, and two interference fringes visible at lower Q values; consistent with a multilayer structure but with a finite small number of bilayers. In this case the data are best described by a model incorporating a discrete number of layers, in this case seven; which include an initial monolayer and three bilayers beneath the monolayer (see table 1).

(iv) Surface phase behaviour

The variation in the surface structure with C_{14}MES and AlCl_3 concentrations is encapsulated in an approximate surface phase diagram, as illustrated in figure 5.

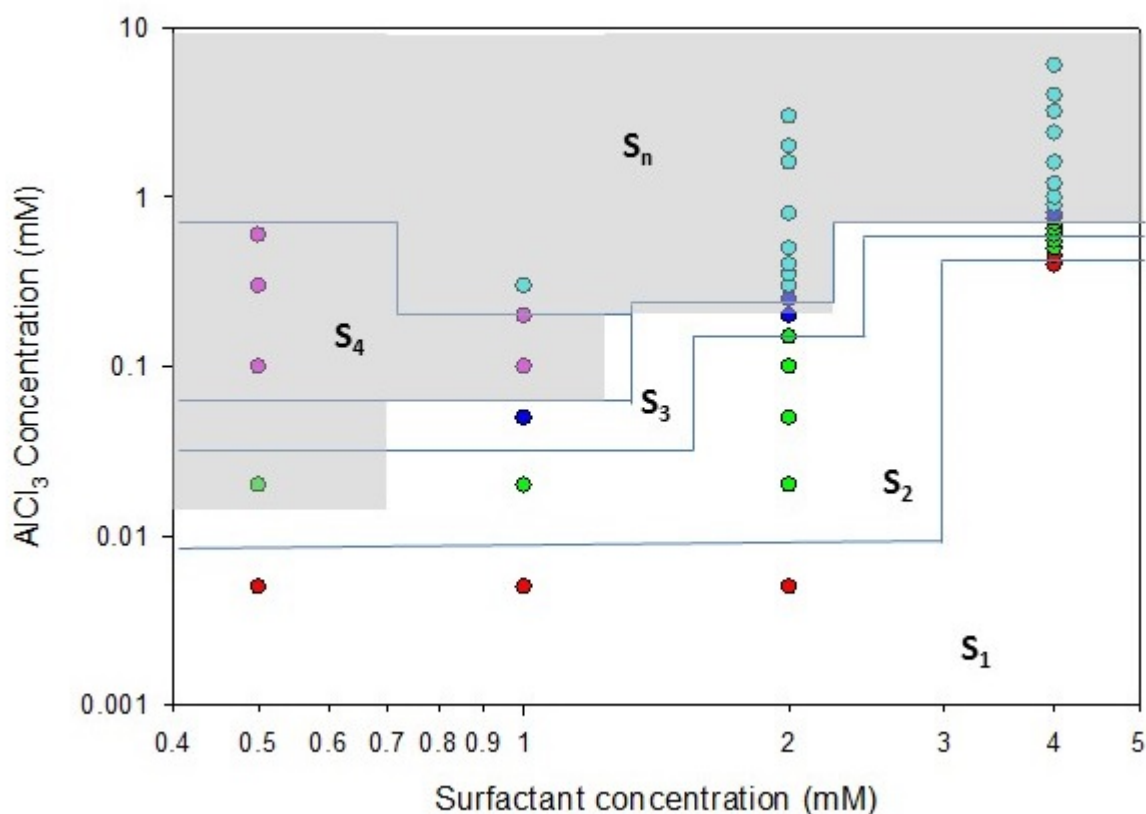


Figure 5. Surface phase behaviour as a function of C_{14}MES and AlCl_3 concentrations. The data points illustrate the points at which NR measurements were made, and the colour coding

is just to distinguish the different structures, S_1 etc. The nomenclature describing the different surface structures is the same as that used in reference 39: that is S_1 is a monolayer, S_2 is a monolayer + bilayer, S_3 is a monolayer+2 bilayers, S_4 is a monolayer + 3 bilayers, and S_n is a multilayer where the number of layers, n , is large. The lines are only approximate boundaries between the different structural regions, but are more a guide to the eye. The grey shaded region represents the region where the samples are cloudy / turbid, and below that region the sample are optically clear. The axes are on a log scale to improve clarity.

The evolution in the surface structure with increasing AlCl_3 concentration is qualitatively similar across the surfactant concentration range studied. That is, a surface with initially a surface monolayer evolves into a surface with a discrete small number of bilayers beneath the monolayer to a multilayer structure with a large number of bilayers at the higher AlCl_3 concentrations. The exception to this is at the lowest surfactant concentration measured, 0.5 mM, where over the AlCl_3 concentration range studied only surface structures with a finite small number of bilayers was observed. At all the surfactant concentrations studied there is a region where surface multilayers with 1 to 3 bilayers beneath the initial monolayer are observed. At the lowest surfactant concentrations studied, 0.5 and 1 mM, there is an additional surface phase present, with 3 distinct bilayers beneath the initial monolayer. This has not been previously observed in the other surface multilayer structures reported for LAS and SLES (29-35). It is not clear at present what the particular criteria are for the formation of the different surface structures. There are no clear quantitative trends in the relative surfactant / electrolyte concentration ratio which determines the evolution in the surface structure, apart from the observation that the amount of AlCl_3 required to induce the different surface phases increases as the surfactant concentration increases. This may, however, in part be due to the relative coarseness of the variation in surfactant and electrolyte concentrations at which NR measurements have been made. However we speculate that there is no particular reason why the structures observed should be especially energetically favoured over any other structures with a finite discrete number of bilayers at the interface. That others have not been generally observed may be simply due to the range of AlCl_3 concentrations over which they are stable being relatively narrow. We also observe that there is no strong correlation between the change in the appearance of the solution, from clear to cloudy / turbid, and the onset of the surface multilayer formation. Indeed the surface layering often occurs before the transition in the solution appearance. However, by the time the surface multilayers with large n are formed the

solutions are usually cloudy. We will return to these points later in the general discussion that follows.

(v) Discussion

The conditions for lamellar formation, L_α , in solution occur when the Israelachvili, Mitchell and Ninham packing parameter (48), $pp=v/al$, where v is the volume, l the extended length of the hydrophobic unit and a is a cross-sectional area, is between 0.5 and 1.0. This condition is usually satisfied at high surfactant concentrations or with the addition of electrolyte when the electrostatic screening has reduced a sufficiently for pp to be in the range 0.5 to 1.0, and a space filling lamellar phase forms, $L_\alpha(sf)$. In di-chain surfactants this criterion can often be fulfilled at relatively low surfactant concentrations. The increase in pp is also generally associated with a reduction in the preferred curvature to form planar structures. The addition of multivalent ions, Ca^{2+} , Al^{3+} , to an anionic surfactant reduces a and increases pp more effectively but often then results in precipitation; the problem associated with detergency in hard water (8-12). However, in some systems attractive forces exist which result in the formation of a swollen lamellar phase, $L_\alpha(sw)$, or a concentrated lamellar phase, $L_\alpha(c)$, in coexistence with a dilute solution. The origins of the attractive force were reviewed recently by Thomas and Penfold (39). Here the strong binding and complexation of the Al^{3+} ions to the $C_{14}MES$ surfactant reduces the area / molecule at the surface and drives the formation of the surface multilayer structures observed. In this case the surface provides a template or attractive force to promote the formation or adsorption of a concentrated lamellar phase at the interface, and it can be likened to a wetting or pre-wetting transition.

Although the surface layering phenomena was observed for the anionic surfactant LAS with the addition of Ca^{2+} ions (30-32), only monolayer adsorption was observed with the addition of Ca^{2+} to the anionic surfactant SLES (33-35). The stronger binding of Al^{3+} was required to promote surface multilayer formation with SLES. This was attributed to the more weakly anionic nature of SLES compared to LAS, which is manifest in a stronger Na^+ counterion binding and lower level of dissociation for SLES. As such the stronger complexation associated with Al^{3+} compared to Ca^{2+} was required to displace the Na^+ counterion and drive surface lamellar formation. For the $C_{14}MES$ data presented here the addition of Ca^{2+} also only promotes an increase in the adsorption, and does not drive the transition from monolayer to multilayer adsorption. This only occurs for $C_{14}MES$ with the addition of Al^{3+} . The ST and isotherm data presented for $C_{14}MES$ (29) are, as discussed earlier, consistent with a relatively weakly ionic

surfactant; weaker than LAS or SDS, and comparable to SLES. Hence the observations are entirely consistent with those reported for SLES in the presence of Ca^{2+} and Al^{3+} .

Kashchiev and Exerowa (49) have estimated the surface tension of a free bilayer to be $\sim 1\text{mN/m}$. Compared to that the adsorption of the initial monolayer at the surface, S_1 , reduces the surface tension substantially. Hence there has to be significant coupling to the monolayer to drive the formation of additional layers at the interface. This coupling can occur through aspects of the structure, electrostatic interactions or bridging. It is assumed here that the Al^{3+} binds to neighbouring surfactant ions within the plane of the surfactant layer to reduce the area/molecule and preferred curvature, and to bridge across layers to provide the attractive force for lamellar formation. This was previously argued as the mechanism for the formation of the surface multilayers with the anionic surfactant SLES (34); where it was shown that changes in the ethylene oxide group of the SLES molecule disrupted the packing and ability the bridge across layers. Alargova et al (6) showed that the onset of micelle growth in SLES solutions with the addition of AlCl_3 coincided with the parameter, ξ , where $\xi = (C_s - \text{cmc}) / Z_m C_m$, C_s is the surfactant concentration, Z_m and C_m the valency and concentration of counterions, was ≤ 1.0 . That is, the counterion charge is in excess. From the previous discussion by Xu et al (34, 35), and the earlier discussions here on the ratio of Al^{3+} / surfactant concentrations coinciding with the different structural transitions, the criterion of Alargova et al (6) is clearly not a sufficient requirement for the onset of the surface layering.

A common feature of the systems that form the surface multilayer structures induced by multivalent counterions is that the surface structures form at low surfactant concentrations and in the regime before precipitation occurs in solution or before phase separation to form $L_\alpha(c)$ in solution. This is what in part has prompted the analogy with wetting and pre-wetting. It implies that the nature of the interaction energy, ΔG , that drives the addition of an initial bilayer, S_2 , subsequent bilayers, S_3 , S_4 etc, and to multilayer formation, S_n , is not sufficiently strong that the bulk phase separation occurs; and hence this is why the adsorption of S_2 , S_3 etc and S_n has been likened to pre-wetting and wetting transitions.

In general the surface structural features that are nearly always observed as a function of Al^{3+} concentration are the initial monolayer, S_1 , structures with a single bilayer, S_2 , and the extended multilayer structures, S_n . Whether more intermediate surface phases, such as S_3 , S_4 etc with increasing numbers of bilayers, are observed depends very much upon the relative surfactant and Al^{3+} concentrations and the surfactant structure. This implies that the addition of the first

bilayer to form S_2 is a relatively strong pre-wetting transition, and that the formation of S_m above a critical Al^{3+} concentration also has a relatively strong driving force and is associated with a wetting transition. This further implies that which intermediate structures, S_3 , S_4 etc, are formed and observed will depend upon relatively subtle changes in the conditions and hence the coupling between the layers, and may not always be captured by the relatively coarse grid of Al^{3+} and surfactant concentrations explored.

The NR measurements were made using deuterium labelled surfactants which are more dense than the solution, and so the wetting or pre-wetting description is entirely appropriate. Precipitation in solution is not observed and the appearance of the different surface structures do not strongly correlate with the transition from clear to cloudy / turbid solutions. Although the timescale for the surface structures to reach equilibrium is relatively slow it is not associated with precipitation. Typically the surface structures can take ~ 2 to 3 hrs to reach their steady state or equilibrium, as determined from repeated NR measurements until the reflectivity profiles no longer change with time, as illustrated in figure 3. Furthermore the timescale for the surface to reach a steady state does depend upon the eventual surface structure that evolves. For example, the adsorption of a surface monolayer, S_1 , only is rapid, and occurs on a timescale which is instantaneous compared to the measurement time. The evolution of the surface multilayer structure, S_n , where n is large, has the slowest timescale and takes typically up to ~ 3 hrs; and the timescale for the formation of the intermediate surface structures, S_2 , S_3 etc, is intermediate between those two extremes.

As previously reported (37) the formation of surface multilayer structures is accompanied by pronounced and persistent wetting of hydrophobic surfaces. This could have important consequences for many of the potential applications of these systems.

CONCLUSIONS

ST and NR have been used to study the adsorption properties of an anionic surfactant, methyl ester sulfonate, which has the potential for improved detergency, biodegradability and biocompatibility (16-28). NR data have established the nature of the adsorption isotherm and the response of the adsorption to electrolyte in the regime where monolayer adsorption is observed (29). The ST and NR data are consistent with a relatively weakly ionic surfactant, with properties similar to SLES and LAS and much weaker than SDS (33, 34). As observed with LAS and SLES the greater tolerance towards precipitation in the presence of multivalent ions is an indication of the tendency to form multilayer structure at the interface. In the presence

of Ca^{2+} only monolayer adsorption is observed, as was reported also for SLES (34, 35), and this is attributed to the greater Na^+ binding associated with those more weakly ionic surfactants. In the presence of Al^{3+} surface multilayer formation is observed due to the strong surfactant / Al^{3+} binding or complexation; and a wider range of surface structures, compared to SLES (34, 35), is observed. The results, coupled with the previous observations for SLES, indicate that the tolerance to precipitation in the presence of multivalent ions and the weakly ionic nature of the surfactant appear to be the important criteria associated with surface multilayer formation at low surfactant concentrations. This is an important extension of the earlier studies on SLES (34, 35), and for a different surfactant structure provides a further insight into the criteria for multilayer adsorption. The surface multilayer structures and their potential for enhanced surface delivery of a range of active agents, and the unusually strong wetting properties in the presence of low concentrations of Al^{3+} ions offer great potential for a wide range of applications of the MES surfactants.

ACKNOWLEDGEMENTS

The provision of beam time on the INTER reflectometer at ISIS is acknowledged. The invaluable scientific and technical assistance of the Instrument Scientists and support staff is greatly appreciated.

REFERENCES

- (1) J. J. Scheibel, The evolution of anionic surfactant technology to meet the requirements of the laundry detergent industry, *J. Surf. Deter.* 2004, 7, 319-328
- (2) Y. U. Yangxin, Z. Jin, A. E. Bayley, Development of surfactants and builders in detergent formulations, *Chinese J. Chem. Eng.* 2008, 16, 517-527
- (3) J. F. Scamehorn in *Phenomena in mixed surfactant systems*, Ed J. F. Scamehorn, ACS Symp. Ser. 311, ACS, Washington DC, 1988
- (4) M. Rosen in *Phenomena in mixed surfactant systems*, Ed J. F. Scamehorn, ACS Symp. Ser. 311, ACS, Washington DC, 1988
- (5) A. Sein, J. B. F. N. Engberts, E. van der Linden, J. van der Pas, Lyotropic phases of dodecylbenzene sulfonates with different counterions in water, *Langmuir*, 1996, 12, 2913-2923
- (6) R. G. Alargova, K. D. Danov, J. T. Petkov, P. A. Kralchevsky, P. A. Broze, A. Mahreteab, Sphere-to-rod transition in the shape of anionic micelles determined by surface tension measurements, *Langmuir*, 1997, 13, 5544-5551
- (7) P. J. Missel, N. A. Mazer, M. C. Carey, G. B. Benedek, Influence of alkali-metal counterions on the sphere to rod transition in alkyl sulfate micelles, *J. Phys. Chem.* 1989, 93, 8354-8360
- (8) K. L. Steller, J. F. Scamehorn, Surfactant precipitation in aqueous solutions containing mixtures of anionic and nonionic surfactants, *J. Am. Oil Chem. Soc.* 1986, 63, 566-574
- (9) P. Paton-Morales, F. I. Talens-Aleson, Effect of ionic strength and competitive adsorption of Na^+ on the flocculation of Lauryl sulfate micelles with Al^{3+} , *Langmuir*, 2001, 17, 6059-6064
- (10) B. L. Chou, J. H. Bae, Surfactant precipitation and redissolution in brine, *J. Coll. Int. Sci.* 1983, 96, 192-203
- (11) J. F. Scamehorn, S. D. Christian, R. T. Ellington, in *Surfactant based separation processes*, J. F. Scamehorn, J. H. Harwell Eds. Surfactant Science Series, Marcel Dekker, New York, 1989, Vol 33
- (12) P. Somasundaran, K. P. Ananthapadmanabhan, M. S. Celik, Precipitation – redissolution phenomena in sulfate – AlCl_3 solutions, *Langmuir*, 1988, 4, 1061-1063

- (13) R G Alargova, K D Danov, P A Kralchevsky, G Broze, A Mahreteab, Growth of giant rodlike micelles of ionic surfactants in the presence of Al^{3+} counterions, *Langmuir*, 1998, 14, 4036-4049
- (14) R G Alargova, V P Ivanova, P A Kralchevsky, A Mahreteab, G Broze, Growth of rodlike micelles in anionic surfactant solutions in the presence of Ca^{2+} counterions, *Coll. Surf. A*, 1998, 142, 201-218
- (15) J H Mu, G Z Li, Rheology of viscoelastic anionic micellar solutions in the presence of multivalent counterions, *Coll. Polym. Sci.* 2001, 279, 872-875
- (16) K D Danov, R D Stanimirova, P A Kralchevsky, E S Basheva, V I Ivanova, J T Petkov, Sulfonated methyl esters of fatty acids in aqueous solution: interfacial and micellar properties, *J. Coll. Int. Sci.* 2015, 457, 307-318
- (17) Z A Maurad, R Ghazali, P Siwayanan, Z Ismail, S Ahmad, Alpha-sulfonated methyl ester as an active ingredient in palm based powder detergents, *J. Surf. Det.* 2006, 9, 161-166
- (18) L Cohen, F Soto, A Melgarejo, D W Roberts, Performance of Φ -sulfo fatty methyl ester sulfonate versus linear alkyl benzene sulfonate, secondary alkane sulfates, and α -sulfo fatty methyl ester sulfonate, *J. Surf. Det.* 2008, 11, 181-186
- (19) D W Roberts, Aquatic toxicity – are surfactant properties relevant, *J. Surf. Det.* 2000, 3, 309-315
- (20) R Ghazali, Z A Maurad, P Siwayanan, M Yusof, A Ahmad, Assessment of aquatic effects of palm-based alpha-sulfonated methyl esters (SME), *J. Oil. Palm Res.* 2006, 18, 225-230
- (21) R Ghazali, A Ahmad, Biodegradability and ecotoxicity of palm stearin based methyl ester sulfonates, *J. Oil Palm Res.* 2004, 16, 39-44
- (22) R Ghazali, The effect of disalt on the biodegradability of methyl ester sulfonates (MES), *J. Oil Palm Res.* 2002, 14, 45-50
- (23) S Ahmad, P Siwayanan, H A Murad, H A Aziz, H Seng Soi, Beyond biodiesel, methyl esters as the route for the production of surfactant feed stocks, *Inform*, 2007, 18, 216-220
- (24) L Cohen, F Trujillo, Synthesis, characterisation and surface properties of sulfonated methyl esters, *J. Surf. Det.* 1998, 1, 335-341
- (25) L Cohen, F Soto, M S Imura, Separation and extraction of Φ -methyl ester sulfonates: new features, *J. Surf. Det.* 2001, 4, 73-74

- (26) W Stein, H Baumann, α -sulfonated fatty acids and esters: manufacturing process, properties and applications, JAOCS, 1975, 52, 323-329
- (27) K Ohbu, M Fujiwara, Y Abe, Physicochemical properties of α -sulfonated fatty acid esters, Prog. Coll. Polym. Sci. 1998, 109, 85-92
- (28) S P Wong, W H Lim, S F Cheng, C H Chuah, Properties of sodium methyl ester α -sulfo alkylate / trimethyl ammonium bromide mixtures, J. Surfact. Deterg. 2012, 15, 601-611
- (29) R K Thomas, J Penfold, H Xu, P X Li, K Ma, D W Roberts, J T Petkov, R Welbourn, Adsorption of methyl ester sulfonate at the air-water interface: can limitations in the application of the Gibbs equation be overcome by 'computer purification', Langmuir, 2017, 33, 9944-9953
- (30) J Penfold, R K Thomas, C C Dong, I Tucker, K Metcalfe, S Golding, I Grillo, Equilibrium surface adsorption behaviour in complex anionic / nonionic surfactant mixtures, Langmuir, 2007, 23, 10140-10149
- (31) J Penfold, R K Thomas, C C Dong, I Tucker, K Metcalfe, S Golding, C Gibson, I Grillo, Surface and solution properties of anionic / nonionic surfactant mixtures of alkylbenzene sulfate and triethylene glycol decyl ether, Langmuir, 2010, 26, 10614-10626
- (32) J Penfold, R K Thomas, C C Dong, I Tucker, K Metcalfe, S Golding, C Gibson, I Grillo, The adsorption and self-assembly of mixtures of alkylbenzene sulfate isomers and the role of divalent electrolyte, Langmuir, 2011, 27, 6674-6684
- (33) J T Petkov, I M Tucker, J Penfold, R K Thomas, D N Petsev, C C Dong, S Golding, I Grillo, The impact of multivalent counterions Al^{3+} on the surface adsorption and self-assembly of the anionic surfactant alkyloxyethylene sulfate and anionic / nonionic surfactant mixtures, Langmuir, 2010, 26, 16691-16709
- (34) H Xu, J Penfold, R K Thomas, J T Petkov, I Tucker, J R P Webster, The formation of surface multilayers at the air-water interface from sodium polyethylene glycol monoalkyl ether sulfate / $AlCl_3$ solutions: the role of the size of the polyethylene oxide group, Langmuir, 2013, 29, 11656-11666
- (35) H Xu, J Penfold, R K Thomas, J T Petkov, I Tucker, J R P Webster, The formation of surface multilayers at the air-water interface from sodium polyethylene glycol monoalkyl ether sulfate / $AlCl_3$ solutions: the role of alkyl chain length, Langmuir, 2013, 29, 11744-11753

- (36) H Xu, J Penfold, R K Thomas, J T Petkov, I Tucker, J R P Webster, I Grillo, A Terry, Ion specific effects in trivalent counterion induced surface and solution self-assembly of the anionic surfactant sodium polyethylene glycol monododecyl ether sulfate, *Langmuir*, 2014, 30, 4094-4702
- (37) J Penfold, R K Thomas, P X Li, H Xu, I M Tucker, J T Petkov, D S Sivia, Multivalent counterion induced surfactant multilayer formation at hydrophobic and hydrophilic solid-solution interfaces, *Langmuir*, 2015, 31, 6773-6781
- (38) R Bradbury, J Penfold, R K Thomas, I M Tucker, J T Petkov, C Jones, Enhanced perfume delivery to interfaces using surface multilayer structures, *J. Coll. Int. Sci.* 2016, 463, 199-206
- (39) R K Thomas, J Penfold, Multilayering of surfactant systems at the air-water dilute aqueous solution interface, *Langmuir*, 2014, 31, 7440-7456
- (40) J Webster, S Holt, R Dalglish, INTER: the chemical interfaces reflectometer on target station 2 at ISIS, *Physica B*, 2006, 385-386, 1164-1166
- (41) J R Lu, R K Thomas, J Penfold, Surfactant layers at the air-water interface: structure and composition, *Adv. Coll. Int. Sci.* 2000, 84, 143-304
- (42) Taylor, D. J. F.; Thomas, R. K.; Penfold, J. Polymer- surfactant interactions at the air-water interface, *Adv. Coll. Int. Sci.* **2007**, 132, 69-110
- (43) Y Jin, S Tian, J Guo, X Ren, X Li, S Gao, Synthesis, characterisation and exploratory application of anionic surfactant fatty acid methyl ester sulfonate from waste cooking oil, *J Surf. Deter.* 2016, 19, 467-475
- (44) H Xu, K Ma, PX Li, R K Thomas, J Penfold, J R Lu, Limitations in the application of the Gibbs equation to anionic surfactants at the air-water interface: SDS and SLES above and below the cmc, *Langmuir*, 2013, 29, 9335-9351
- (45) O S Heavens, *Optical properties of thin solid films*, Dover, New York, 1991
- (46) I M Tidswell, B M Ocko, P S Pershan, S R Wasserman, G M Whitesides, J D Axe, X-ray specular reflection studies on silicon coated by organic monolayers (alkylsiloxanes), *Phys. Rev. B* 1990, 41, 1111-1128
- (47) S K Sinha, M K Sanyal, S K Satija, C F Majkrzak, D A Neumann, H Homma, S Szpala, H Gibaud, H Morkov, X-ray scattering studies from surface roughness of GaAs / AlAs multilayers, *Physica B* 1994, 198, 72-77

- (48) J N Israelachvili, D J Mitchell, B W Ninham, Theory of self-assembly of hydrocarbon amphiphiles into micelles and bilayers, *J. Chem. Soc. Faraday Trans. 2*, 1976, 72, 1525-1568
- (49) D Kashchiev, D E Exerowa, Structure and surface energy of the surfactant layers in the Alveolar surface, *Eur. J. Biophys.* 2001, 30, 34-41

SUPPLEMENTARY INFORMATION

The impact of electrolyte on the adsorption of the anionic surfactant methyl ester sulfonate at the air-solution interface: surface multilayer formation.

H Xu, R K Thomas, J Penfold, P X Li, K Ma, R J L Welbourne, D W Roberts, J T Petkov

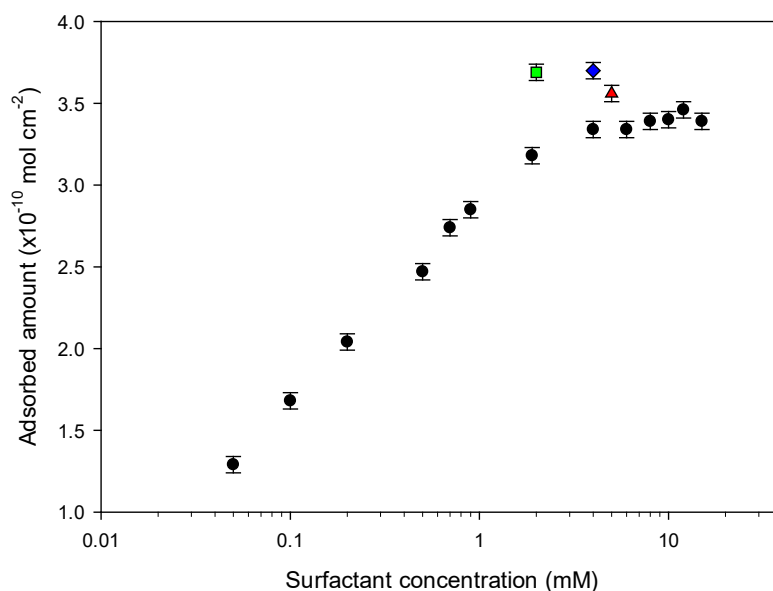


Figure S1. Adsorbed amount for $C_{14}MES$ versus surfactant concentration (●), (■) 2mM $C_{14}MES$ / 2 mM $CaCl_2$, (◆) 4mM $C_{14}MES$ / 0.4 mM $AlCl_3$, (▲) 5 mM $C_{14}MES$ / 100 mM $NaCl$.

For clarity the data point at 2.9 mM is not included, as in the preceding paper by Xu et al (ref 29 in main Text) it is argued that the adsorption at 2.9 mM is anomalous due to residual impurities.